



Thermal physiology and species distribution models reveal climate vulnerability of temperate amphibians

Alyssa A. Gerick^{1†}, Robin G. Munshaw^{1†}, Wendy J. Palen^{1*†},
Stacey A. Combes² and Sacha M. O'Regan¹

¹Department of Biological Sciences, Earth to Ocean Research Group, Simon Fraser University, Burnaby, BC V5A 1S6, Canada,
²Concord Field Station, Department of Organismic and Evolutionary Biology, Harvard University, Cambridge, MA 02138, USA

ABSTRACT

Aim High-latitude ectotherms are predicted to be less physiologically vulnerable to climate warming than tropical species based on their larger thermal safety margins, the distance between ambient temperatures and species' thermal optima. We sought to test the prediction that high latitude amphibians are buffered against the impacts of climate warming.

Location British Columbia, Canada.

Methods We estimated the risk from climate change for three high-latitude amphibian species (*Spea intermontana*, *Rana aurora* and *Pseudacris regilla*) by combining thermal performance experiments with species distribution models and predicted changes in maximum summer temperatures through the 2080s, in order to demonstrate temporal and geographical trends in vulnerability to climate warming among and within species.

Results We found that species have thermal safety margins of 3.2–3.8 °C based on current maximum summer temperatures. However, by the 2080s (emissions scenario A1B), we estimate that 45–82% of our focal species' current distributions will experience maximum summer temperatures above their thermal optima. We also found that by using long-term average temperatures, as some studies have done, there were almost no scenarios in which populations of any species were experiencing temperatures greater than their thermal optima.

Main conclusions Combining spatially explicit species distribution models with performance physiology allows us to predict where limiting temperatures will occur in the coming decades, and can guide climate mitigation and conservation efforts before populations decline. Despite moderate thermal safety margins, high-latitude ectotherms can be highly vulnerable to climate warming when spatio-temporal variation is incorporated into estimates of risk as a result of climate change.

Keywords

Ecological niche models, global climate change, *Pseudacris regilla*, *Rana aurora*, *Spea intermontana*, thermal physiology.

*Correspondence: W. J. Palen, 8888 University Drive, Burnaby, BC, V5A 1S6, Canada.

E-mail: wpalen@sfu.ca

†These authors share equally in first authorship.

INTRODUCTION

Anthropogenic climate change is arguably the largest threat faced by contemporary ecosystems (Thomas *et al.*, 2004). Changing temperatures have initiated a global redistribution of species (Thomas, 2010; Sunday *et al.*, 2012) and threaten an increasing fraction of global biodiversity (Thuiller *et al.*, 2005; Aitken *et al.*, 2008). Climate impacts are expected to

vary spatially and temporally, and species' responses can be individualistic (Walther *et al.*, 2002), challenging the development of mechanistic predictions of risk. Recent advances have combined thermal physiology with estimates of future ambient temperatures to predict the climate vulnerability of ectotherms (Thomas *et al.*, 2004, 2012; Deutsch *et al.*, 2008; Tewksbury *et al.*, 2008; Huey *et al.*, 2009; Kolbe *et al.*, 2010; Sinervo *et al.*, 2010; Angert *et al.*, 2011).

Ectotherm thermal physiology has been well studied over the past half-century. Short-term measures of thermal performance relative to optimum temperatures have been correlated with differences in predation risk, fecundity and population growth rates (Fry & Hart, 1948; Huey & Kingsolver, 1989; Watkins, 1996; Schulte *et al.*, 2011). Thermal performance curves (TPCs) express the relationship between locomotion and temperature (Watkins, 1996; Köhler *et al.*, 2011). From these curves, several useful analytical metrics can be extracted: thermal performance optima (T_{opt}), critical thermal maxima (CT_{max}), critical thermal minima (CT_{min}), and thermal performance breadths (T_{br} ; Huey & Stevenson, 1979). Such measures are related to a suite of factors including evolutionary history, climate and life-history traits (Andrews & Schwarzkopf, 2012). When TPCs are combined with future temperatures, climate vulnerability can be estimated by calculating thermal safety margin (TSM; degrees between habitat temperature and T_{opt}) or warming tolerance (WT; degrees between habitat temperature and CT_{max} ; Deutsch *et al.*, 2008). Consequently, studies of TPCs across many taxa have led to global predictions of the relative climate vulnerability of ectotherms to future warming (Tewksbury *et al.*, 2008; Huey *et al.*, 2009; Clusella-Trullas *et al.*, 2011; Duarte *et al.*, 2012; Kellermann *et al.*, 2012), where species at low latitudes will be more vulnerable than those at higher latitudes (Deutsch *et al.*, 2008; Tewksbury *et al.*, 2008; Duarte *et al.*, 2012). These studies suggest that warm, consistent temperatures result in the narrow T_{br} of equatorial ectotherms, which also occupy thermal environments closer in their T_{opt} resulting in smaller TSMs. By comparison, more variable temperatures experienced by temperate ectotherms result in broad T_{br} , and these species occupy much cooler thermal environments than T_{opt} , resulting in larger TSMs. This suggests that temperate species may be buffered or even benefit from climate warming as they move closer to T_{opt} (Deutsch *et al.*, 2008). These studies provide the first mechanistic basis for predicting ecological consequences of climate warming for ectotherms on a global scale. However, many global analyses characterize environmental temperatures from single or few locations per species, which may not be representative of the range experienced by populations across heterogeneous environments. Further, researchers have called for analyses based on predictions of extreme temperature events instead of long-term average performance or temperature measurements, because extreme temperatures are expected to drive acute physiological effects (Kingsolver *et al.*, 2011; Schulte *et al.*, 2011; Buckley & Kingsolver, 2012).

Here we estimated the climate vulnerability of three temperate ectotherms at the northern extent of their ranges: Great Basin spadefoot toad, *Spea intermontana* (Cope, 1883), northern red-legged frog; *Rana aurora* Baird & Girard, 1852; and Pacific chorus frog, *Pseudacris regilla* (Baird & Girard, 1852). We estimated thermal optima using swimming performance experiments, then complemented these results with species distribution models (SDMs) to estimate what proportion of species' current ranges will exceed their thermal optima across a range of future climate scenarios. When

compared to latitudinal-based predictions of vulnerability, we hypothesized that SDMs would better capture spatial variability in temperature experienced by populations across their range, possibly resulting in higher thermal vulnerability, and that the proportion of species distributions exceeding T_{opt} would be likewise higher when based on maximum expected temperatures.

MATERIALS AND METHODS

We empirically estimated thermal performance curves for aquatic larvae of three pool-breeding amphibians native to the Pacific coast of North America: *S. intermontana*, *R. aurora* and *P. regilla*. Maximum velocity (V_{max}) and acceleration (A_{max}) during 1 second of burst swimming were used as the basis for constructing thermal performance curves. Larval stages of pool-breeding anurans are expected to be particularly susceptible to changes in thermal conditions because they are restricted to shallow aquatic environments, are temporally constrained to grow to metamorphosis during ice-free months, and their small body size renders them isothermal with the environment (Lutterschmidt & Hutchison, 1997). We combined thermal performance measures (T_{opt}) with maximum entropy (MaxEnt; Phillips *et al.*, 2006) species distribution models and regionally downscaled climate change predictions to estimate where and when these high-latitude species are expected to exceed their thermal optima in future decades.

Natural history and species sampling

We collected embryos of *R. aurora*, *S. intermontana* and *P. regilla* from one to three populations at the northern extent of each species' range in British Columbia, Canada, including wetlands within the Lower Seymour Conservation Reserve (49°15'02.97" N, 123°00'49.28" W), Pinecrest wetlands (50°01'56.96" N, 123°07'17.76" W), White Lake Grasslands Protected Area (49°16'04.43" N, 119°35'48.18" W), and the University of British Columbia (UBC) Endowment Lands (49°15'02.97"N, 123°14'17.25" W). The three focal species span the range of life history characteristics exhibited by northern anurans. *Rana aurora* is a cold-adapted coastal species with slow developmental rates and the lowest CT_{min} of ranid embryos in North America (COSEWIC, 2004). In contrast, *S. intermontana* has the shortest larval development period of anura in North America (COSEWIC, 2007), and is a habitat specialist in the thermally variable Great Basin desert. *Pseudacris regilla* exhibits intermediate developmental timing, and exploits the widest range of habitat types, suggesting a high level of adaptability (Schaub & Larsen, 1978).

Physiological assays

Embryos were reared under common outdoor conditions, and larvae were housed separately by species in plastic wading pools containing pond water and leaf litter from their

source locations. Larvae were transferred indoors into 38L glass aquaria containing dechlorinated tap water and leaf litter at ambient temperature (*c.* 15 °C) when larvae reached Gosner stage 37 (Watkins & Vraspir, 2006). Tadpoles remained indoors for the remainder of the experiment and were euthanized at the conclusion of performance assays.

Submersible aquarium heaters (100–200 W) and a recirculating chilled water bath were used to generate temperature treatments ranging from 5 °C up to the maximum possible temperature prior to observing substantial mortality (see Appendix S1a in Supporting Information). Tadpoles were randomly assigned to temperature treatments after *c.* 72 h at room temperature, and acclimatized to temperature treatments over the course of 2–24 h. Tadpoles were stocked at constant densities that varied slightly by species based on the number of available larvae (8 of *R. aurora*, 16 of *S. intermontana*, 12 of *P. regilla* per aquaria), as individual larvae were only tested at a single temperature. Larvae remained in temperature treatments for 96 h before being tested in burst swimming performance trials. Individual tadpoles were tested in a 40-cm long v-shaped Plexiglas (© Altuglas Intl.) channel filled with < 2 cm of water. We chose to measure acute responses (96 h) to test the immediate physiological effects of temperature incubations, as opposed to chronic adaptive effects observed in longer-term exposures (Bennett & Huey, 1990). Burst swimming was recorded using a high-speed video camera (Casio ZR-100, 240 fps) suspended directly over the raceway, and a startle response was generated with a weak electrical pulse (S88 Grass Stimulator) using silver-tipped electrodes on either side of the tadpole's tail (10 V for *R. aurora*, 20 V for *P. regilla*, and 40 V for *S. intermontana*; Wilson & Franklin, 1999). Following swimming trials, tadpoles were photographed for measurement of snout-to-vent (SVL) and tail length. Tadpoles were run only once each, and all trials were conducted early in the day (between 10:00 and 14:00 h).

Raw body position data were processed with a 5th order high-pass Butterworth filter (Winter, 2009) in MATLAB, to smooth out frame-to-frame errors in localizing body position. The dominant frequency of motion was generated by tail beat frequency, which varied widely between tadpoles at different temperatures. As such, we filtered each video using a customized cutoff frequency that was 3 Hz above the measured tail beat frequency (cutoff = $f_{\text{tail}} + 3$ Hz). Velocity was calculated as the distance travelled between adjacent frames divided by the period (1/frame rate), and acceleration calculated as the difference in velocity between frames divided by the period. We identified the maximum velocity and maximum acceleration during the first second, excluding the first 25 ms, where motion initiation sometimes results in a vertical asymptote. We excluded trials with visual quality issues (water reflection) or erratic tadpole behaviour (i.e. errors in stimulus application) and selected the five clearest tadpole recordings from each temperature treatment for further analysis. Nonlinear locally weighted least squares (LOESS; Zuur *et al.*, 2009) regression models were fitted to data points for each species separately (R Development Core

Team, 2005). To reduce the selection bias present in measuring the performance of only those animals that survived, we assigned a performance of zero to animals that died in each temperature treatment, then weighted our LOESS models by the proportion of mortalities in each treatment (Appendix S1). The temperature at maximal physiological performance (T_{opt}) was estimated from best model fits for each of two measured response variables, maximum velocity (V_{max}) and maximum acceleration (A_{max}), by solving the model for the maximum estimated value across the range of temperatures tested, and thermal breadth calculated as the range of temperatures over which swimming performance exceeded 80% of performance at T_{opt} (Huey & Stevenson, 1979).

MaxEnt climate modelling

To estimate probabilistic regional distributions for each of our three focal species, we constructed maximum entropy (MAXENT; Phillips *et al.*, 2006) species distribution models (SDMs) from species occurrence data and 19 bioclimatic variables available from the WorldClim database version 1.4 (Hijmans *et al.*, 2005), a digital elevation map (DEM, British Columbia Geographic Warehouse; <http://pub.data.gov.bc.ca/>), aspect and slope derived from DEM (using ARCGIS 10; ESRI, Redlands, CA, USA), and percentage tree cover (DeFries *et al.*, 2000), similar to previously reported methodologies (Kumar & Stohlgren, 2009). All variables were re-sampled to 500 m × 500 m resolution to maintain consistent detail in complex coastal areas. Following Kumar & Stohlgren (2009), we checked for multicollinearity among all variables by testing for cross-correlations at 1000 random points within the distribution mapping area. We only included one variable of each highly correlated pair (Pearson's correlation coefficient; $r > 0.75$) in the model, resulting in 15 variables being used to train our distribution models. For each focal species, we assembled occurrence data at the northern extent of each species' range in British Columbia (arbitrarily defined as north of the Canada–USA border; *R. aurora*: $n = 99$, *S. intermontana*: $n = 81$, *P. regilla*: $n = 304$) from the Biodiversity Information Facility (<http://data.gbif.org/>), the BC Conservation Data Center (<http://www.env.gov.bc.ca/cdc/>), and NatureWatch (<http://www.naturewatch.ca/>). Occurrences with locational uncertainty (represented by polygons) were reduced to a single point at the centroid. Our SDMs were created under the assumption that the arbitrarily chosen Canadian–USA border used to delimit the northern extent of each species' range is an acceptably biologically relevant partition that subdivides the focal northern populations from the remaining distribution of each species, a method which can increase local model accuracy (Gonzalez *et al.*, 2011). We used MAXENT 3.3.3k (<http://www.cs.princeton.edu/~schapire/maxent/>) to create probability maps of habitat suitability for each species using pseudo-absence points chosen to a prevalence of 0.5 (number of occurrences/number of occurrences + number of pseudo-absences). We limited the delineation of each species' current distribution to areas with a probability of predicting suitable

habitat (MAXENT logistic output) equal to or greater than the prevalence value, and randomly generated 1000 localities within each species' range using Geospatial Modelling Environment (<http://www.spatialecology.com/gme/>).

Climate warming scenarios

At each of the 1000 random localities within each species' modelled distribution, we extracted two habitat temperature metrics from future climate forecasts (Hijmans *et al.*, 2005), mean quarterly summer air temperature ($T_{\text{hab-ave}}$) and mean maximum monthly air temperature (May–August; $T_{\text{hab-max}}$), for each of three time periods in the future (2020s, 2050s, 2080s) across a range of emissions scenarios (A1B, A2, B2; IPCC, 2000) and global circulation models (CGCM3.1, CGCM2.0, MK3.0, MK2.0, HadCM3; downscaled using the delta method). For each time period and each emissions scenario, temperature metrics ($T_{\text{hab-ave}}$: average temperature of summer quarter, and $T_{\text{hab-max}}$: average of monthly maximum temperatures for May–August) were averaged across all global circulation models (GCMs).

Based on T_{opt} determined for each species from the physiological performance assays (for both V_{max} and A_{max}), we calculated TSMs for each species using current climate (1950–2000), and predicted how TSMs will change as $T_{\text{hab-ave}}$ and $T_{\text{hab-max}}$ within each species' range (1000 localities from above) change in future decades (2020s, 2050s, 2080s) under a range of emissions scenarios (A1B, A2, B2). We used ArcGIS 10 to map predicted TSMs (based on A_{max}) for scenario A1B during the 2020s to visualize the spatial pattern of expected thermal vulnerability for each species, as the three collectively span a broad range of life histories and thermal geographies. A detailed description of the emissions scenarios examined and justification for focusing on a single scenario and performance metric can be found in Appendix S2. Similarly, to compare the relative vulnerability of species across future climates, we calculated what fraction of the 1000 localities within each species' present-day range is expected to exceed T_{opt} when using maximum monthly summer temperatures ($T_{\text{hab-max}}$) versus mean summer temperatures ($T_{\text{hab-ave}}$). We tested whether or not current TSMs were different through bootstrap resampling of the 1000 random

localities generated for each species. For each species, we sampled 100 of the localities with replacement, calculated the mean value, then saved the difference of each comparison of species means (e.g. median Species 1 – median Species 2). We replicated this process 1000 times, and then examined the 95% confidence interval (CI) of each permutation distribution of differences to determine if any comparisons were significantly different from 0.

RESULTS

Physiological assays

Thermal performance curves generated from individual swimming trials conducted across a range of temperatures (5–35.5 °C) show that the three species differ in thermal performance (Table 1). Estimates of thermal optima (T_{opt}) based on both response variables were similar within species (range: 22.1–26.3 °C), with *R. aurora* having the lowest T_{opt} , and *S. intermontana* and *P. regilla* with T_{opt} approximately 2–4 °C higher (Table 1). We estimated that *S. intermontana* had the widest T_{br} (V_{max} 16.6, A_{max} 12.2 °C), followed by *R. aurora* (V_{max} 14.3, A_{max} 9.3 °C) and *P. regilla* (V_{max} 9.7, A_{max} 8.3 °C). We identified a slightly different ranking among the three species in maximum swimming speed (*S. intermontana* = 30.7 cm/s, *P. regilla* = 29.3 cm/s, and *R. aurora* = 27.5 cm/s; Table 1, Appendix S3), and acceleration; with *R. aurora* on average achieving the fastest A_{max} (1381.0 cm/s²), followed by *S. intermontana* (1360.5 cm/s²) and *P. regilla* (1288.7 cm/s²; Table 1, Fig. 1).

MaxEnt climate modelling

We fit probabilistic SDMs using occurrence data from the northern extent of each species' range and a range of bioclimatic variables. Resulting SDMs highlight large geographical differences in species distributions that coincide with differences in climate vulnerability for each species (estimated below). Fitted models provided good predictive power as described by the area under the receiver operating characteristic curve (AUC; Phillips *et al.*, 2006; *R. aurora*: 0.989, *S. intermontana*: 0.991, *P. regilla*: 0.976).

Table 1 Peak performance values for maximum acceleration (A_{max}) and maximum velocity (V_{max}) calculated from fitted thermal performance curves for *Spea intermontana*, *Rana aurora* and *Pseudacris regilla* populations in British Columbia, Canada. T_{br} is the breadth of temperature over which 80% or greater of maximum performance is achieved, T_{opt} is the estimated peak performance temperature for each response variable.

Response variable	Species	T_{br} (min, max; °C)	T_{opt} (°C)	Maximum performance	Snout–vent length (mm ± 95% CI)
V_{max}	<i>S. intermontana</i>	16.6 (15.6, 32.2)	25.1	30.7 cm/s	16.56 ± 0.44
	<i>R. aurora</i>	14.3 (13.6, 27.9)	22.1	27.5 cm/s	15.08 ± 0.62
	<i>P. regilla</i>	9.7 (19.1, 28.9)	24.6	29.3 cm/s	10.57 ± 0.29
A_{max}	<i>S. intermontana</i>	12.2 (20.0, 32.2)	26.3	1360.5 cm/s ²	
	<i>R. aurora</i>	9.3 (18.2, 27.5)	22.8	1381.0 cm/s ²	
	<i>P. regilla</i>	8.3 (20.4, 28.7)	24.8	1288.7 cm/s ²	

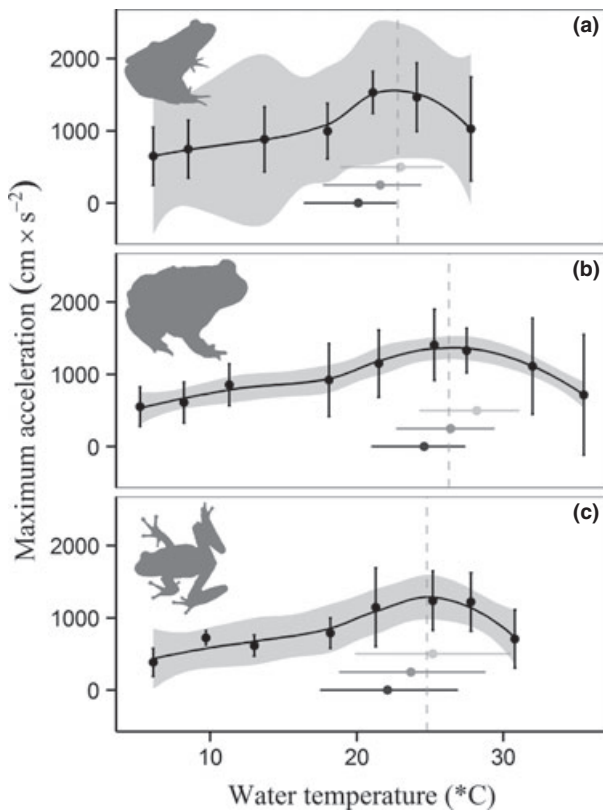


Figure 1 Thermal performance curves generated from maximum acceleration (A_{\max}) measured for larvae of (a) *Rana aurora*, (b) *Spea intermontana*, and (c) *Pseudacris regilla* populations in British Columbia, Canada. Points along each curve represent mean A_{\max} (\pm 95% CI) at each temperature treatment, and dashed vertical lines represent estimates of each species' performance optimum. Horizontal bars represent the mean (\pm 95% CI) of expected environmental temperatures within each species' distribution in the 2020s (black), 2050s (dark grey), and 2080s (light grey) using the A1B emissions scenario and mean maximum monthly air temperature (May–August) ($T_{\text{hab-max}}$) ($n = 5$ for each temperature treatment).

Climate warming scenarios

We sampled 1000 random localities within each species' estimated MaxEnt distribution ($> 50\%$ probability of suitable habitat) to characterize the spatial variation in past (1950–2000) and expected future (2020–2080) temperatures for each species over a range of climate scenarios (A1B, A2, B2). Temperatures experienced over the past half-century highlight differences among the three species' current thermal geography, based on average (mean of $T_{\text{hab-ave}}$; *R. aurora* = 15.1, *P. regilla* = 16.4, *S. intermontana* = 17.3 °C) and maximum summer temperatures (mean of $T_{\text{hab-max}}$; *S. intermontana* = 23.1, *R. aurora* = 19.1, *P. regilla* = 21.0 °C; Appendix S1b). Environmental temperatures at the same locations for future decades (A1B scenario) demonstrate that differences among species' thermal geography are expected to increase, especially for maximum summer temperatures ($T_{\text{hab-max}}$; Appendix S1b).

Estimates of environmental temperatures were combined with estimates of T_{opt} (A_{\max}), and used to calculate mean TSMs (\pm 95% CI) for past, as well as future decades (A1B scenario, Table 2). Over the past half-century, species had mean TSMs between 2.0 and 3.8 °C using $T_{\text{hab-max}}$ (7.0–9.0 °C using $T_{\text{hab-ave}}$). By the 2080s, all species are predicted to have uniformly negative TSMs (–0.2 to –1.9 °C), where TSMs were eroded at a rate of approximately 0.5 °C per decade (range: 0–1.2 °C) for all three species regardless of whether calculated based on $T_{\text{hab-ave}}$ or $T_{\text{hab-max}}$ (Table 2). When we map predictions of future TSMs ($T_{\text{hab-max}}$, scenario A1B; Fig. 2), we find strong geographical variation in predicted climate vulnerability. *Rana aurora* is predicted to exhibit a longitudinal trend in TSMs by the 2020s (Fig. 2a), with populations on the west coast of Vancouver Island predicted to have relatively high TSMs with values declining to zero and below in the east. *Spea intermontana* is restricted to a smaller and more interior distribution, and we found that TSM in the 2020s depended on elevation, with negative TSMs in lower elevation valley-bottom populations (Fig. 2b). *Pseudacris regilla* exhibits a longitudinal trend similar to that of *R. aurora*, where temperatures experienced by inland populations are close to or beyond T_{opt} by the 2020s compared to cooler coastal and island populations (Fig. 2c).

When we calculated the percentage of localities that are predicted to exceed T_{opt} (Appendix S1c) in future decades (using A_{\max} and scenario A1B) as a continuous measure of the spatial heterogeneity in climate vulnerability, we found that our estimates were strongly influenced by the choice of temperature metric ($T_{\text{hab-ave}}$ or $T_{\text{hab-max}}$) for all three species. Thermal vulnerability estimated using $T_{\text{hab-ave}}$ results in only a small fraction (5%) of the northern range of *P. regilla*, and none of the ranges of *R. aurora* or *S. intermontana*, experiencing temperatures exceeding T_{opt} by the 2080s (Fig. 3, lower planes; Appendix S1c). By contrast, when future climate vulnerability was estimated using $T_{\text{hab-max}}$, we predicted that a large proportion of all three species' distributions would experience thermally limiting conditions ($> T_{\text{opt}}$; Fig. 3, upper planes), ranging between 45% and 82% by the 2080s. The differences between $T_{\text{hab-ave}}$ and $T_{\text{hab-max}}$ were particularly large for *S. intermontana*.

DISCUSSION

We identified a high degree of risk posed by future temperature changes to three temperate ectotherms at the northern extent of their ranges. The risk posed to each species depends on how the biogeography of each species' spatial distribution and differences in their thermal physiology intersect with spatially explicit predictions of temperature changes. We predict that all three amphibian species are likely to experience thermally limiting conditions in the coming decades based on how maximum temperatures will change in space and time (Figs 2 & 3). All three species currently have similar TSMs (using $T_{\text{hab-max}}$, A_{\max} ; 3.2–3.8 °C), which provide a physiological buffer in the face of ambient temperature

Table 2 Thermal safety margins (TSMs), calculated for current and future climates across three emissions scenarios for *Spea intermontana*, *Rana aurora* and *Pseudacris regilla* populations in British Columbia, Canada.

Scenario	Species	Response variable	Thermal safety margin, °C (95% CI)					
			2020s		2050s		2080s	
			$T_{\text{hab-max}}$	$T_{\text{hab-ave}}$	$T_{\text{hab-max}}$	$T_{\text{hab-ave}}$	$T_{\text{hab-max}}$	$T_{\text{hab-ave}}$
A1B	<i>S. intermontana</i>	V_{max}	0.5 (−2.4–4.1)	7.5 (4.0–10.4)	−1.3 (−4.3–2.4)	5.9 (2.0–9.1)	−3.1 (−6.0–0.8)	4.3 (−0.3–7.8)
		A_{max}	1.7 (−1.1–5.3)	8.7 (4.2–11.6)	−1.9 (−3.1–3.6)	7.1 (3.2–10.3)	−1.9 (−4.8–2.0)	5.5 (0.9–9.0)
	<i>R. aurora</i>	V_{max}	2.0 (−0.6–5.7)	5.9 (4.0–8.5)	0.5 (−2.3–4.4)	4.3 (2.3–7.1)	−0.9 (−3.8–3.2)	2.8 (0.3–5.8)
		A_{max}	2.7 (0.1–6.4)	6.6 (4.7–9.2)	1.2 (−1.6–5.1)	5.0 (2.9–7.8)	−0.2 (−3.1–3.9)	3.5 (1.0–6.5)
	<i>P. regilla</i>	V_{max}	2.5 (−2.3–7.1)	5.9 (3.1–9.2)	0.9 (−4.2–5.8)	4.0 (0.6–7.7)	−0.6 (−5.9–4.7)	2.3 (−1.9–6.3)
		A_{max}	2.7 (−2.1–7.3)	6.1 (3.3–9.4)	1.1 (−4.0–6.0)	4.2 (0.8–7.9)	−0.4 (−5.7–4.9)	2.5 (−1.7–6.5)
A2	<i>S. intermontana</i>	V_{max}	0.6 (−2.2–4.3)	7.7 (4.2–10.6)	−0.6 (−3.8–3.0)	6.6 (3.1–10.1)	−2.4 (−5.4–1.3)	4.8 (0.6–8.5)
		A_{max}	1.8 (−1.0–5.5)	8.9 (5.4–11.8)	0.6 (−2.4–4.2)	8.1 (4.3–11.3)	−1.2 (−4.2–2.5)	6.0 (1.8–7.7)
	<i>R. aurora</i>	V_{max}	2.1 (−0.4–5.8)	4.7 (4.2–8.7)	1.1 (−1.5–4.6)	3.9 (3.0–7.6)	−0.3 (−3.1–3.2)	1.9 (1.0–6.2)
		A_{max}	2.8 (0.3–6.5)	5.4 (4.9–9.4)	1.8 (−0.8–5.3)	4.6 (3.7–8.3)	0.4 (−2.4–3.9)	2.6 (1.7–7.0)
	<i>P. regilla</i>	V_{max}	2.6 (−2.2–7.2)	6.0 (3.3–9.2)	1.5 (−3.5–6.2)	4.7 (1.9–7.9)	−0.1 (−5.3–4.9)	2.8 (−0.4–6.6)
		A_{max}	2.8 (−2.0–7.4)	6.2 (3.5–9.4)	1.7 (−3.3–6.4)	4.9 (2.1–8.1)	0.1 (−5.1–5.1)	3.0 (−0.2–6.8)
B2	<i>S. intermontana</i>	V_{max}	0.3 (−2.6–4.0)	6.6 (2.7–10.2)	−0.6 (−3.6–3.1)	6.9 (3.2–10.3)	−1.4 (−4.4–2.2)	6.0 (2.2–9.9)
		A_{max}	1.5 (−1.4–5.2)	8.1 (3.9–11.4)	0.6 (−2.4–4.3)	8.1 (4.4–11.5)	−0.2 (−3.2–3.4)	7.2 (3.4–11.1)
	<i>R. aurora</i>	V_{max}	1.9 (−0.7–5.5)	5.8 (3.8–8.5)	2.0 (−1.6–4.8)	5.0 (2.7–7.8)	0.4 (−2.3–4.0)	4.2 (1.6–7.0)
		A_{max}	2.6 (0.0–6.0)	6.5 (4.5–9.2)	2.7 (−0.9–5.5)	5.7 (3.4–8.5)	1.1 (−1.6–4.7)	4.9 (2.3–7.7)
	<i>P. regilla</i>	V_{max}	2.3 (−2.6–7.0)	5.8 (3.0–9.1)	1.5 (−3.6–6.4)	4.7 (1.6–8.1)	0.8 (−4.3–5.7)	3.8 (0.7–7.4)
		A_{max}	2.5 (−2.4–7.2)	6.0 (3.2–9.3)	1.7 (−3.4–6.6)	4.9 (1.8–8.3)	1.0 (−4.1–5.9)	4.0 (0.9–7.6)

Scenario	Species	Response variable	Current thermal safety margin, °C (95% CI)	
			$T_{\text{hab-max}}$	$T_{\text{hab-ave}}$
Current	<i>S. intermontana</i>	V_{max}	2.0 (−0.9–5.5)	7.8 (5.1–10.9)
		A_{max}	3.2 (0.3–6.7)	9.0 (6.3–12.1)
	<i>R. aurora</i>	V_{max}	3.0 (0.5–6.5)	7.0 (5.2–9.5)
		A_{max}	3.7 (1.2–7.2)	7.7 (5.9–10.2)
	<i>P. regilla</i>	V_{max}	3.6 (−1.0–7.9)	8.2 (4.9–10.9)
		A_{max}	3.8 (−0.8–8.1)	8.4 (5.1–11.1)

A_{max} , maximum acceleration; V_{max} , maximum velocity; $T_{\text{hab-max}}$, mean maximum monthly air temperature (May–August); $T_{\text{hab-ave}}$, mean quarterly summer air temperature.

changes, but we predict that TSMs will be rapidly eroded at a rate of 0.5 °C per decade. This rate of change leads to a high proportion of each species' range experiencing temperatures above T_{opt} by the 2080s, with 82% of the current distribution of *S. intermontana* and approximately 60% and 45% of *P. regilla* and *R. aurora*, respectively, expected to occur in thermally limiting environments. We used the spatially explicit nature of our SDMs to evaluate geographical patterns of risk and found that populations of each species are at higher risk of deleterious temperatures at lower elevations (*S. intermontana*) and with increasing distance inland from the coast (*R. aurora* and *P. regilla*; Fig. 2).

When species are not able to follow their climate envelope across space as temperatures increase, species persistence depends on whether decreases in the thermal performance of individuals directly reduce population growth rates. We observed moderate rates of mortality (Appendix S1a) as well as physical traits indicating thermal stress (enlarged blood vessels, loss of righting reflex) at extreme high temperatures (Huey & Kingsolver, 1989), suggesting that our highest tem-

perature treatments approached CT_{max} for all three species. Previous work has shown that similar physiological responses among a wide range of ectotherm taxa can translate into reduced population growth rates and be used as the basis for comparisons across species at a global scale (Deutsch *et al.*, 2008). When exposures are sublethal, either higher or lower than T_{opt} , small decreases in physiological performance (e.g. reduced burst swimming velocity or acceleration, or higher tortuosity) may also translate into lower individual survival through the effects of predators.

Both lethal and sublethal thermal effects on larval performance and survival may be buffered by a range of compensatory responses in ectotherms including shifts in species phenology or distributions (Parmesan & Yohe, 2003), behavioural changes (Huey *et al.*, 2012), and plasticity or adaptation (Bennett & Huey, 1990). However, recent work suggests that amphibians may have limited capacity to use many of these compensatory pathways. Some species exhibit only limited thermal plasticity (John-Alder *et al.*, 1988) and reduced potential for thermal acclimation (Niehaus *et al.*, 2011),

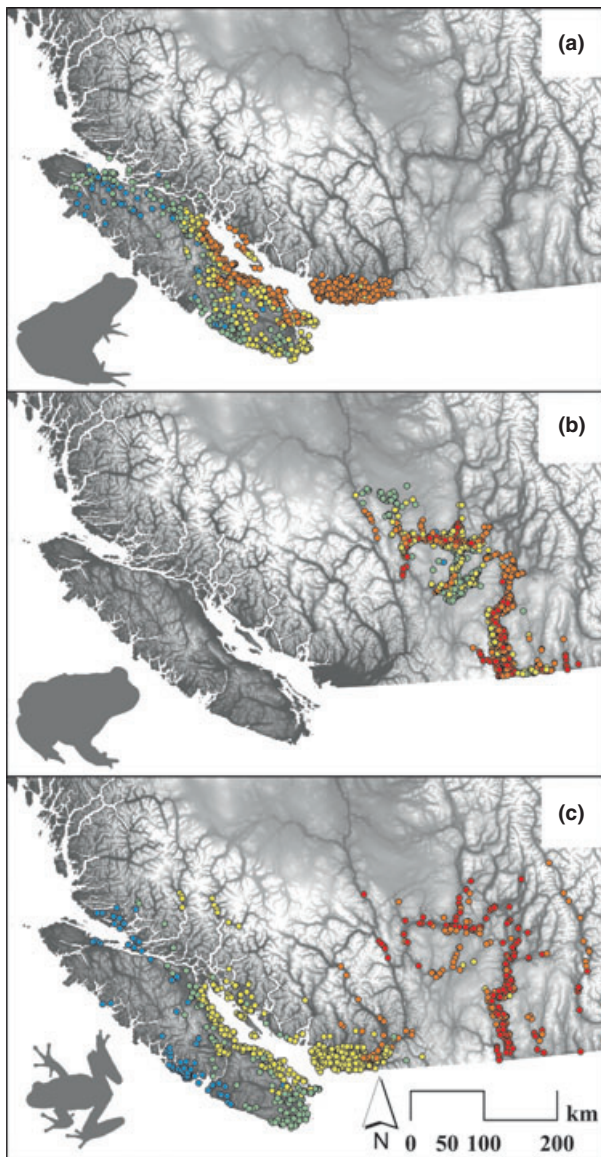


Figure 2 Spatial patterns of range-wide thermal proximity to thermal optima, based on maximum acceleration (A_{\max}) performance during the 2020s under the A1B emissions scenario, using mean maximum monthly air temperature (May–August), $T_{\text{hab-max}}$, for (a) *Rana aurora*, (b) *Spea intermontana*, and (c) *Pseudacris regilla* populations in British Columbia, Canada. Colours represent the magnitude of thermal safety margin ($^{\circ}\text{C}$): red < 0 , orange = 0–2, yellow = 2–4, green = 4–6, blue > 6 . Points represent randomly selected localities at which thermal geography predictions were characterized.

suggesting that amphibians may not have the capacity to keep pace with climate warming once outside of historical thermal regimes. Similarly, observations of compensatory shifts in breeding timing due to climate warming have been limited in amphibians (Gibbs & Breisch, 2001; but see Beebee, 1995), which may be critically important for species that exhibit temperature dependent breeding (Popescu & Gibbs, 2009). In the case of our study system, the potential for amphibians at high

latitudes to shift reproductive timing is tightly constrained by the short summer season and a rigid development schedule that requires reaching a threshold size for metamorphosis in one season (Laurila *et al.*, 2002), as species do not typically survive the winter as larvae. When considered together, these data suggest that amphibians possess limited capacity to respond to climate warming, and such vulnerability may be compounded in the presence of additional stressors such as novel pathogens and habitat destruction (Pounds *et al.*, 2006).

Global analyses of ectotherm climate vulnerability have predicted that species at higher latitudes should be physiologically buffered against climate warming because of larger thermal safety margins compared to tropical species (Huey *et al.*, 2009; Duarte *et al.*, 2012; but see Crozier & Dwyer, 2006). Here we tested the validity of this prediction for three species of amphibians at the northern extent of their ranges, and found that all three species are predicted to be highly vulnerable to future thermal conditions in the coming century. We hypothesized that this discrepancy could be generated by two common features of latitudinal and global-scale analyses of the vulnerability to climate change of ectotherms. First, thermal environments characterized by temperature averages (monthly, quarterly, yearly) are likely to underestimate the frequency of thermally limiting conditions for ectotherms by homogenizing physiologically important temperature variations in time (Fig. 4; *sensu* Buckley & Kingsolver, 2012). Second, collapsing the full range of thermal variation experienced by multiple populations across species' ranges into a single species average similarly underestimates the frequency of thermally limiting conditions in space (Kelly *et al.*, 2012). We recognize that estimating thermal performance curves from a limited subset of populations of each species in British Columbia may limit the geographical scope of this study. However, population-level estimations of thermal performance curves do not differ from species-level estimations for some species (Angert *et al.*, 2011), so our estimates are not likely to be biased by the potential of local cold-adapted populations in cooler climates.

We found strong support that calculations of risk based on $T_{\text{hab-max}}$ and $T_{\text{hab-ave}}$ result in drastically different estimates of species' TSMs, with much higher predictions of risk (smaller TSMs) when based on $T_{\text{hab-max}}$. These results highlight that the degree of temperature averaging in time can generate large differences in predictions of climate. Recent literature has suggested that extreme high temperatures may better characterize thermal limits compared to ambient averages due to the acute impacts of thermal stress on organism and population function (Smith, 2011; Buckley & Kingsolver, 2012). In addition, global climate models predict future increases in the magnitude of annual seasonality (broader range of annual temperatures; IPCC, 2007), suggesting that even when mean annual temperatures increase modestly, increased seasonality may result in a greater frequency and intensity of extreme thermal highs during summer months (Field *et al.*, 2007). Extreme temperature events are often a primary driver of acute thermal impacts on

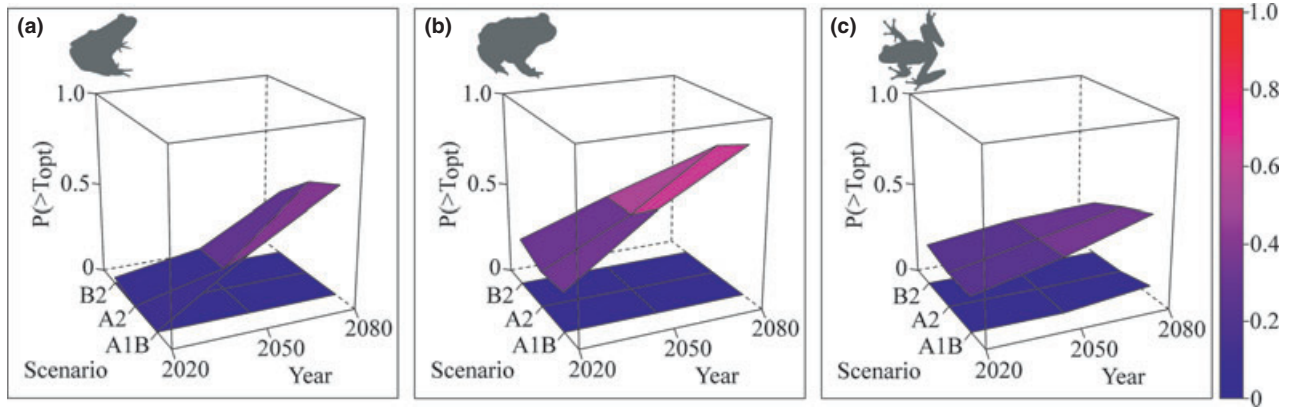


Figure 3 Proportion (P) of the current distribution of (a) *Rana aurora*, (b) *Spea intermontana*, and (c) *Pseudacris regilla* in British Columbia, Canada, expected to experience summer temperatures (upper plane: mean maximum monthly air temperature (May–August), $T_{\text{hab-max}}$; lower plane: mean quarterly summer air temperature, $T_{\text{hab-ave}}$) greater than thermal performance optimum, T_{opt} (for maximum acceleration, A_{max}), across current and future decades and emissions. Scenario A1B is the focus of results presented in the text.

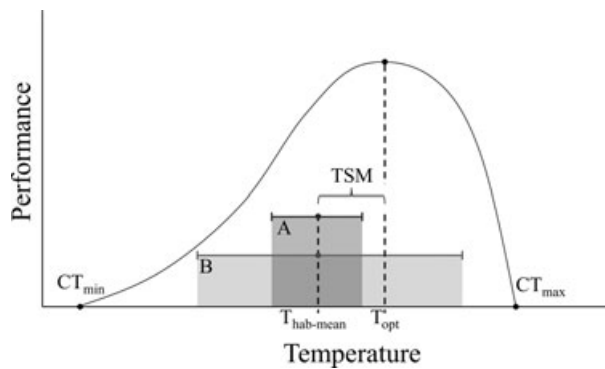


Figure 4 Conceptual model illustrating the role of the mean and variance of thermal safety margin (TSMs) for predicting vulnerability of ectotherms to climate change. For estimate A, mean habitat temperature ($T_{\text{hab-mean}}$) was measured in a few localized habitats, taking into account only a small portion of the species’ thermal geography. For estimate B, $T_{\text{hab-mean}}$ was measured across the species’ range, incorporating the entirety of the species’ thermal geography. Both estimate A and B have the same mean T_{hab} and therefore same TSM, but estimate B shows that a substantial proportion of populations may already be experiencing deleterious effects of temperatures above thermal performance optimum (T_{opt}). CT_{max} , critical thermal maximum; CT_{min} , critical thermal minimum.

individual survival (due in part to the exponential relationship between metabolic rate and temperature; Dillon *et al.*, 2010), especially if they impact vulnerable life-stages (Kingsolver *et al.*, 2011). However, relative extreme temperature events (in the statistical sense) are poorly related to average temperatures (Luber & McGeehin, 2008), suggesting that the relative climate vulnerability of species based on average temperatures may not be a reliable proxy for responses to future climates if extreme temperatures are the primary driver of impacts. Some previous work has used $T_{\text{hab-ave}}$, with the justification that ectotherms are likely to alter their phenology so that increased productivity in the shoulder

seasons compensates for decreased productivity during summer extremes.

We also found strong support for the prediction that large differences in estimated vulnerability to climate change would be generated from the degree of temperature averaging in space. Estimates of mean current TSMs (c. 7–9 °C for $T_{\text{hab-ave}}$, c. 3–4 °C $T_{\text{hab-max}}$) match the general prediction that temperate species should occur in thermal environments well below their T_{opt} and CT_{max} , and such species are expected to be well-buffered from warming (Martin & Huey, 2008). However, when we used SDMs to characterize the distribution of ambient temperatures experienced in 1000 random localities throughout the northern extent of each species’ range in the 2080s, we predicted that a majority of all three species’ distributions would experience maximum summer temperature in excess of their T_{opt} (Fig. 3). This prediction would be different if only a localized subset of populations were considered, as spatially autocorrelated samples can fail to capture the environmental heterogeneity present at larger spatial scales (Fortin *et al.*, 2006). The importance of incorporating spatial variability in temperatures into estimates of climate vulnerability is likely to scale with the climate envelope of individual species, with larger underestimates of risk expected for species that occur across more heterogeneous thermal environments relative to those that occur in more homogenous thermal environments.

Predicting the impacts of anthropogenic stressors prior to population declines and species extinctions is a key objective of modern conservation biology. The global decline in amphibian populations, driven by a diversity of stressors, with many enigmatic declines (Stuart *et al.*, 2004), brings this conservation challenge into stark relief. Our results suggest that the vulnerability of three temperate amphibian species of the Pacific coast of North America, two of which are listed as species at risk in British Columbia (*R. aurora*, *S. intermontana*; COSEWIC, 2004, 2007), may be further exacerbated by increasing environmental temperatures due to global climate

change. In contrast to general predictions of resilience to increasing temperatures in amphibians and other ectotherms at temperate latitudes (Deutsch *et al.*, 2008; Sinervo *et al.*, 2010; Duarte *et al.*, 2012), we find that all three species are expected to experience deleterious thermal environments by mid-century. We found strong support for our hypotheses, that appropriately incorporating modes of thermal variability in both space and time are likely to improve predictions of climate vulnerability, and in this case, dramatically increase estimates of vulnerability to climate change. Were we to evaluate only the mean vulnerability in space using average temperatures rather than maximum, two of the three species we studied would conform to latitudinal predictions of low vulnerability. We further find that species distribution models, although limited by the availability and quality of species occurrence and environmental data, may help to bridge this gap by providing spatially explicit predictions of vulnerability to climate change that may be useful for climate mitigation strategies or conservation decision-making. Our results suggest that accurately assessing vulnerability to climate change for individual species will require describing patterns of macro- (regional and latitudinal) as well as micro- (local) climate attributes, physiological tolerance, potential for adaptability and dispersal, as well as the ecological and physiological trade-offs that are inherent among them but poorly understood.

ACKNOWLEDGEMENTS

The authors thank J. Sunday for helpful comments and feedback; R. Murray, H. Gehrels, C. Moore and B. Mackinnon for field and laboratory assistance; B. Leighton, H. More, M. Donelan and SFU Animal Care staff for logistical support; T. Hedrick for video technical support; D. Schluter for access to the UBC Pond Facility; C. Gerick and Lindair Services for help constructing performance assay equipment; and M. Weston, S. Ashpole, M. Fish and J. Malt for providing information on regional breeding sites. This study was conducted under Simon Fraser University animal care protocol 1006B-11 and British Columbia Ministry of Environment wildlife research permit VII2-76706, and funded by NSERC and the Canada Research Chairs Program.

REFERENCES

- Aitken, S.N., Yeaman, S., Holliday, J.A., Wang, T. & Curtis-McLane, S. (2008) Adaptation, migration or extirpation: climate change outcomes for tree populations. *Evolutionary Applications*, **1**, 95–111.
- Andrews, R.M. & Schwarzkopf, L. (2012) Thermal performance of squamate embryos with respect to climate, adult life history, and phylogeny. *Biological Journal of the Linnean Society*, **106**, 851–864.
- Angert, A.L., Sheth, S.N. & Paul, J.R. (2011) Incorporating population-level variation in thermal performance into predictions of geographic range shifts. *Integrative and Comparative Biology*, **51**, 733–750.
- Baird, S.F. & Girard, C. (1852) Descriptions of new species of reptiles, collected by the U.S. Exploring Expedition, under the command of Capt. Charles Wilkes, U.S.N. *Proceedings of the Academy of Natural Sciences of Philadelphia*, **6**, 174–177.
- Beebee, T.J.C. (1995) Amphibian breeding and climate. *Nature*, **374**, 219–220.
- Bennett, A.F. & Huey, R.B. (1990) Studying the evolution of physiological performance. *Oxford surveys in evolutionary biology*, Vol. 6 (ed. by D.T. Futuyama and J. Antonovics), pp. 251–284. Oxford University Press, Oxford.
- Buckley, L.B. & Kingsolver, J.G. (2012) Functional and phylogenetic approaches to forecasting species' responses to climate change. *Annual Review of Ecology, Evolution, and Systematics*, **43**, 205–226.
- Clusella-Trullas, S., Blackburn, T.M. & Chown, S.L. (2011) Climatic predictors of temperature performance curve parameters in ectotherms imply complex responses to climate change. *The American Naturalist*, **177**, 738–751.
- Cope, E.D. (1883) Notes on the geographical distribution of Batrachia and Reptilia of western North America. *Proceedings of the Academy of Natural Sciences of Philadelphia*, **35**, 10–51.
- COSEWIC (2004) *COSEWIC assessment and update status report on the red-legged frog Rana aurora in Canada*. Committee on the Status of Endangered Wildlife in Canada, Ottawa.
- COSEWIC (2007) *COSEWIC assessment and update status report on the great basin spadefoot Spea intermontana in Canada*. Committee on the Status of Endangered Wildlife in Canada, Ottawa.
- Crozier, L. & Dwyer, G. (2006) Combining population-dynamic and ecophysiological models to predict climate-induced insect range shifts. *The American Naturalist*, **167**, 853–866.
- DeFries, R.S., Hansen, M.C., Townshend, J.R.G., Janetos, A.C. & Loveland, T.R. (2000) A new global 1-km dataset of percentage tree cover derived from remote sensing. *Global Change Biology*, **6**, 247–254.
- Deutsch, C.A., Tewksbury, J.J., Huey, R.B., Sheldon, K.S., Ghalambor, C.K., Haak, D.C. & Martin, P.R. (2008) Impacts of climate warming on terrestrial ectotherms across latitude. *Proceedings of the National Academy of Sciences USA*, **105**, 6668–6672.
- Dillon, M.E., Wang, G. & Huey, R.B. (2010) Global metabolic impacts of recent climate warming. *Nature*, **467**, 704–706.
- Duarte, H., Tejedo, M., Katzenberger, M., Marangoni, F., Baldo, D., Beltrán, J.F., Martí, D.A., Richter-Boix, A. & Gonzalez-Voyer, A. (2012) Can amphibians take the heat? Vulnerability to climate warming in subtropical and temperate larval amphibian communities. *Global Change Biology*, **18**, 412–421.
- Field, C.B., Mortsch, L.D., Brklacich, M., Forbes, D.L., Kovacs, P., Patz, J.A., Running, S.W. & Scott, M.J. (2007) Climate change 2007: impacts, adaptation and vulnerability. *Contribution of Working Group II to the Fourth Assessment*

- Report of the Intergovernmental Panel on Climate Change (ed. by M.L. Parry, O.F. Canziani, J. Palutikof, P.J. van der Linden and C.E. Hanson), pp. 617–652. Cambridge University Press, Cambridge, UK.
- Fortin, M.-J., Dale, M.R.T. & ver Hoef, J. (2006) Spatial analysis in ecology. *Encyclopedia of environmetrics* (ed. by A. El-Shaarawi and W. Piegorisch), pp. 2051–2058. John Wiley & Sons, Ltd, Hoboken, NJ.
- Fry, F.E.J. & Hart, J.S. (1948) Cruising speed of goldfish in relation to water temperature. *Journal of the Fisheries Research Board of Canada*, **7b**, 169–175.
- Gibbs, J.P. & Breisch, A.R. (2001) Calentamiento del clima y fenología de vocalizaciones de ranas cerca de Ithaca, Nueva York, 1900–1999. *Conservation Biology*, **15**, 1175–1178.
- Gonzalez, S., Soto-Centeno, J.A. & Reed, D. (2011) Population distribution models: species distributions are better modeled using biologically relevant data partitions. *BMC Ecology*, **11**, 20.
- Hijmans, R.J., Cameron, S.E., Parra, J.L., Jones, P.G. & Jarvis, A. (2005) Very high resolution interpolated climate surfaces for global land areas. *International Journal of Climatology*, **25**, 1965–1978.
- Huey, R.B. & Kingsolver, J.G. (1989) Evolution of thermal sensitivity of ectotherm performance. *Trends in Ecology and Evolution*, **4**, 131–135.
- Huey, R.B. & Stevenson, R.D. (1979) Integrating thermal physiology and ecology of ectotherms: a discussion of approaches. *American Zoologist*, **19**, 357–366.
- Huey, R.B., Deutsch, C.A., Tewksbury, J.J., Vitt, L.J., Hertz, P.E., Pérez, H.J.Á. & Garland, T. (2009) Why tropical forest lizards are vulnerable to climate warming. *Proceedings of the Royal Society B: Biological Sciences*, **276**, 1939–1948.
- Huey, R.B., Kearney, M.R., Krockenberger, A., Holtum, J.A.M., Jess, M. & Williams, S.E. (2012) Predicting organismal vulnerability to climate warming: roles of behaviour, physiology and adaptation. *Philosophical Transactions of the Royal Society B: Biological Sciences*, **367**, 1665–1679.
- IPCC (2000) *IPCC special report: emissions scenarios*. Cambridge University Press, Cambridge, UK.
- IPCC (2007) *Climate change 2007: the physical science basis. Contribution of Working Group I to the Fourth Assessment Report of the Intergovernmental Panel on Climate Change*. Cambridge University Press, Cambridge, UK.
- John-Alder, H.B., Morin, P.J. & Lawler, S. (1988) Thermal physiology, phenology, and distribution of tree frogs. *The American Naturalist*, **132**, 506–520.
- Kellermann, V., Loeschcke, V., Hoffmann, A.A., Kristensen, T.N., Fløjgaard, C., David, J.R., Svenning, J.-C. & Overgaard, J. (2012) Phylogenetic constraints in key functional traits behind species' climate niches: patterns of desiccation and cold resistance across 95 *Drosophila* species. *Evolution*, **66**, 3377–3389.
- Kelly, M.W., Sanford, E. & Grosberg, R.K. (2012) Limited potential for adaptation to climate change in a broadly distributed marine crustacean. *Proceedings of the Royal Society B: Biological Sciences*, **279**, 349–356.
- Kingsolver, J.G., Woods, H.A., Buckley, L.B., Potter, K.A., MacLean, H.J. & Higgins, J.K. (2011) Complex life cycles and the responses of insects to climate change. *Integrative and Comparative Biology*, **51**, 719–732.
- Köhler, A., Sadowska, J., Olszewska, J., Trzeciak, P., Berger-Tal, O. & Tracy, C.R. (2011) Staying warm or moist? Operative temperature and thermal preferences of common frogs (*Rana temporaria*), and effects on locomotion. *The Herpetological Journal*, **21**, 17–26.
- Kolbe, J.J., Kearney, M. & Shine, R. (2010) Modeling the consequences of thermal trait variation for the cane toad invasion of Australia. *Ecological Applications*, **20**, 2273–2285.
- Kumar, S. & Stohlgren, T.J. (2009) Maxent modeling for predicting suitable habitat for threatened and endangered tree *Canacomyrica monticola* in New Caledonia. *Journal of Ecology and Natural Environment*, **1**, 094–098.
- Laurila, A., Karttunen, S. & Merilä, J. (2002) Adaptive phenotypic plasticity and genetics of larval life histories in two *Rana temporaria* populations. *Evolution*, **56**, 617–627.
- Luber, G. & McGeehin, M. (2008) Climate change and extreme heat events. *American Journal of Preventive Medicine*, **35**, 429–435.
- Lutterschmidt, W.I. & Hutchison, V.H. (1997) The critical thermal maximum: history and critique. *Canadian Journal of Zoology*, **75**, 1561–1574.
- Martin, T.L. & Huey, R.B. (2008) Why “suboptimal” is optimal: Jensen’s inequality and ectotherm thermal preferences. *The American Naturalist*, **171**, E102–118.
- Niehaus, A.C., Wilson, R.S., Seebacher, F. & Franklin, C.E. (2011) Striped marsh frog (*Limnodynastes peronii*) tadpoles do not acclimate metabolic performance to thermal variability. *The Journal of Experimental Biology*, **214**, 1965–1970.
- Parmesan, C. & Yohe, G. (2003) A globally coherent fingerprint of climate change impacts across natural systems. *Nature*, **421**, 37–42.
- Phillips, S.J., Anderson, R.P. & Schapire, R.E. (2006) Maximum entropy modeling of species geographic distributions. *Ecological Modelling*, **190**, 231–259.
- Popescu, V.D. & Gibbs, J.P. (2009) Interactions between climate, beaver activity, and pond occupancy by the cold-adapted mink frog in New York State, USA. *Biological Conservation*, **142**, 2059–2068.
- Pounds, J.A., Bustamante, M.R., Coloma, L.A., Consuegra, J.A., Fogden, M.P.L., Foster, P.N., Marca, E.L., Masters, K.L., Merino-Viteri, A., Puschendorf, R., Ron, S.R., Sánchez-Azofeifa, G.A., Still, C.J. & Young, B.E. (2006) Widespread amphibian extinctions from epidemic disease driven by global warming. *Nature*, **439**, 161–167.
- R Development Core Team (2005) *R: a language and environment for statistical computing*. Version 2.15.3. R Foundation for Statistical Computing, Vienna, Austria. Available at: <http://www.R-project.org/>.
- Schaub, D.L. & Larsen, J.H. (1978) The reproductive ecology of the Pacific treefrog (*Hyla regilla*). *Herpetologica*, **34**, 409–416.

- Schulte, P.M., Healy, T.M. & Fangue, N.A. (2011) Thermal performance curves, phenotypic plasticity, and the time scales of temperature exposure. *Integrative and Comparative Biology*, **51**, 691–702.
- Sinervo, B., Méndez-de-la-Cruz, F., Miles, D.B. *et al.* (2010) Erosion of lizard diversity by climate change and altered thermal niches. *Science*, **328**, 894–899.
- Smith, M.D. (2011) An ecological perspective on extreme climatic events: a synthetic definition and framework to guide future research. *Journal of Ecology*, **99**, 656–663.
- Stuart, S.N., Chanson, J.S., Cox, N.A., Young, B.E., Rodrigues, A.S.L., Fischman, D.L. & Waller, R.W. (2004) Status and trends of amphibian declines and extinctions worldwide. *Science*, **306**, 1783–1786.
- Sunday, J.M., Bates, A.E. & Dulvy, N.K. (2012) Thermal tolerance and the global redistribution of animals. *Nature Climate Change*, **2**, 686–690.
- Tewksbury, J.J., Huey, R.B. & Deutsch, C.A. (2008) Putting the heat on tropical animals. *Science*, **320**, 1296–1297.
- Thomas, C.D. (2010) Climate, climate change and range boundaries. *Diversity and Distributions*, **16**, 488–495.
- Thomas, C.D., Cameron, A., Green, R.E., Bakkenes, M., Beaumont, L.J., Collingham, Y.C., Erasmus, B.F.N., de Siqueira, M.F., Grainger, A., Hannah, L., Hughes, L., Huntley, B., van Jaarsveld, A.S., Midgley, G.F., Miles, L., Ortega-Huerta, M.A., Peterson, A.T., Phillips, O.L. & Williams, S.E. (2004) Extinction risk from climate change. *Nature*, **427**, 145–148.
- Thomas, M.K., Kremer, C.T., Klausmeier, C.A. & Litchman, E. (2012) A global pattern of thermal adaptation in marine phytoplankton. *Science*, **338**, 1085–1088.
- Thuiller, W., Lavorel, S., Araújo, M.B., Sykes, M.T. & Prentice, I.C. (2005) Climate change threats to plant diversity in Europe. *Proceedings of the National Academy of Sciences USA*, **102**, 8245–8250.
- Walther, G.-R., Post, E., Convey, P., Menzel, A., Parmesan, C., Beebee, T.J.C., Fromentin, J.-M., Hoegh-Guldberg, O. & Bairlein, F. (2002) Ecological responses to recent climate change. *Nature*, **416**, 389–395.
- Watkins, T.B. (1996) Predator-mediated selection on burst swimming performance in tadpoles of the Pacific tree frog, *Pseudacris regilla*. *Physiological Zoology*, **69**, 154–167.
- Watkins, T.B. & Vraspir, J. (2006) Both incubation temperature and posthatching temperature affect swimming performance and morphology of wood frog tadpoles (*Rana sylvatica*). *Physiological and Biochemical Zoology*, **79**, 140–149.
- Wilson, R.S. & Franklin, C.E. (1999) Thermal acclimation of locomotor performance in tadpoles of the frog *Limnodynastes peronii*. *Journal of Comparative Physiology B: Biochemical, Systemic, and Environmental Physiology*, **169**, 445–451.
- Winter, D.A. (2009) *Biomechanics and motor control of human movement*. John Wiley & Sons, Hoboken, NJ.
- Zuur, A.F., Ieno, E.N., Walker, N., Saveliev, A.A. & Smith, G.M. (2009) *Mixed effects models and extensions in ecology with R*. Springer, New York, New York.

SUPPORTING INFORMATION

Additional Supporting Information may be found in the online version of this article:

Appendix S1 Additional tables containing experimental mortality data, as well as additional data on current and future predictions about thermal environment.

Appendix S2 Additional methods regarding emissions scenarios and temperature metrics.

Appendix S3 Thermal performance curves generated from maximum burst swimming velocity (V_{\max}) measured for larvae of (a) *Rana aurora*, (b) *Spea intermontana*, and (c) *Pseudacris regilla*.

BIOSKETCH

The lead authors A.A.G., R.G.M. and W.J.P. are part of the Earth to Ocean research group at Simon Fraser University (<http://www.sfu.ca/biology/earth2ocean/Earth2Ocean/Home.html>). This lab group is broadly focused on conservation and the aquatic ecology of aquatic systems from tropical coral reefs to Alaskan rivers and wetlands, as well as their ecological and biophysical links with surrounding ecosystems.

Author contributions: A.A.G., R.G.M. and W.J.P. conceived the ideas; A.A.G. and S.M.O. collected the data; A.A.G., R.G.M. and S.J.C. performed the analysis; A.A.G., R.G.M. and W.J.P. wrote the manuscript.

Editor: Richard Ladle